# Mode locking and Arnold tongues in integrate-and-fire neural oscillators

S. Coombes and P. C. Bressloff
*Nonlinear and Complex Systems Group, Department of Mathematical Sciences, Loughborough University, Leicestershire LE11 3TU, United Kingdom*
(Received 5 February 1999)

An analysis of mode-locked solutions that may arise in periodically forced integrate-and-fire (IF) neural oscillators is introduced based upon a firing map formulation of the dynamics. A $q:p$ mode-locked solution is identified with a spike train in which $p$ firing events occur in a period $q\Delta$, where $\Delta$ is the forcing period. A linear stability analysis of the map of firing times around such solutions allows the determination of the Arnold tongue structure for regions in parameter space where stable solutions exist. The analysis is verified against direct numerical simulations for both a sinusoidally forced IF system and one in which a periodic sequence of spikes is used to induce a biologically realistic synaptic input current. This approach is extended to the case of two synaptically coupled IF oscillators, showing that mode-locked states can exist for some self-consistently determined common period of repetitive firing. Numerical simulations show that such solutions have a bursting structure where regions of spiking activity are interspersed with quiescent periods before repeating. The influence of the synaptic current upon the Arnold tongue structure is explored in the regime of weak coupling. [S1063-651X(99)09207-7]

PACS number(s): 87.10+e, 05.45.Xt

## I. INTRODUCTION

It has long been known that nerve membranes can exhibit exotic responses to periodic stimulation, whether it be in the form of a smooth alternating current [1] or the injection of current pulses [2]. Among the most commonly observed and studied behaviors are mode-locked states in which a repetitive regular output is entrained to some multiple of the forcing period. In addition to mode-locked rhythms it is often possible to observe irregular or aperiodic rhythms in which entrainment is nonexistent [3]. Interestingly, for many biological oscillators the stable behaviors which are most commonly observed correspond to low-order ratios between the number of cycles of forcing and the subsequently generated rhythm. Moreover, the stable rhythms can be organized in a regular fashion such that aperiodic motion is often generated in regions of parameter space separating rhythmic behavior [2,3]. Rhythmic behavior is also produced by many neural systems in the absence of a pacemaker signal. Neurons communicate by firing and transmitting action potentials. Commonly, in response to a constant applied stimulus, action potentials occur in a periodic fashion. However, many cell types exhibit more complex behavior characterized by brief bursts of oscillatory activity interspersed with quiescent periods. The swimming and heartbeat networks of the medicinal leech, the swimming network of the pelagic mollusc, the feeding network of the freshwater snail, and the gastric network of the crustacean stomatogastric ganglion are all examples of central pattern generators of the above type [4]. When a wave form of bursting activity is present it is natural to use the taxonomy of mode locking to classify possible rhythms. Rhythmic solutions may be distinguished by the number of intraburst events within a period of oscillation. Since neural membranes generate brief electrical pulses or spikes, a theory of mode locking in both driven neurons and networks of neurons must necessarily relate output spike trains to incoming synaptic currents. In this paper we focus on the integrate-and-fire (IF) oscillator as a model neuron that submits to an exhaustive analysis of all mode-locked states. Moreover, with the introduction of an IF Liapunov exponent we are also able to probe any apparent aperiodic or chaotic behavior.

In Sec. II we introduce the dynamics of an IF oscillator and consider the construction of a map of the firing times of the oscillator in response to an arbitrary periodic input signal. The conditions under which this map reduces to the lift of a degree one circle map are discussed in detail. Although much is known about mode-locked behavior in circle maps (see Ref. [5] for a discussion of smooth circle maps and Ref. [6] for a review of piecewise linear models) the firing times for an IF oscillator are determined as a set of threshold crossings so that standard tools of dynamical systems theory are not so easily applied. At the heart of this paper is the notion of a mode-locked state and its realization in an IF dynamical system. By introducing a set of firing phases and considering the period of the output spike train to be rationally related to the period of forcing, we show how to describe such dynamical behavior using an implicit map of the firing times. If $p$ spikes are fired within a window of time that is $q$ times the input period (for integer $q$), the resulting train is shown to have an average firing rate of $p/q$ and is called a $q:p$ mode-locked state. By considering perturbations of the firing times and considering how they would evolve under a linearization of the full nonlinear IF dynamics, we obtain conditions for the linear stability of mode-locked solutions. The same analysis is used to define the borders of regions in parameter space where stable mode-locked solutions exist (the Arnold tongue structure). Since analytic results about mode-locked solutions can be readily obtained in the limit of zero forcing and can be shown to persist into the regime of nonzero forcing, we consider numerical continuation as a natural means of constructing the full Arnold tongue structure. To complete this theoretical prelude we discuss the notion of Liapunov exponents in discontinuous dynamical systems, and use the

 

recently introduced notion of IF Liapunov exponent [7] to classify IF dynamics as periodic, aperiodic, or chaotic. Section III illustrates the theory of mode locking in driven IF systems for both sinusoidal forcing and forcing with a biologically plausible train of synaptic pulses. In both cases Arnold tongues are constructed and compared against direct numerical integration of the IF equations of motion. In Sec. IV we consider the extension of this work to cover a pair of pulse-coupled IF oscillators that can sustain mode-locked behavior in the absence of any periodic forcing. Based upon earlier work of the authors (see Ref. [8] for a review), we show that the architectures capable of supporting mode-locked solutions with bursting patterns are those with a mixture of excitatory and inhibitory coupling. For the case of pure excitatory or pure inhibitory coupling, the mode-locked solutions typically have a simpler structure that is most readily analyzed in the limit of weak coupling. We end with a brief discussion in Sec. V.

## II. INTEGRATE-AND-FIRE DYNAMICS

The IF oscillator may be regarded as a caricature of a real neuron that captures some essence of its firing or spiking properties. Indeed, the IF model may be obtained as a reduction of the biologically realistic Hodgkin-Huxley equations that have been so successfully applied to the study of excitable nerve tissue [9]. The IF model considered in this paper (often referred to as the leaky IF oscillator) is a model of a leaky, current-clamped membrane in terms of a state variable $U(t)$ (membrane potential), a decay constant $\tau$, and an applied signal $A(t)$. The output of the oscillator is a sequence of firing events that are defined as those times at which $U(t)$ reaches some threshold. Immediately after a firing event the state variable is reset to some resting level. The evolution of the state variable between firing events is prescribed by a smooth dynamical system which may or may not be linear. Of course the system as a whole is nonlinear due to the effects of the resetting mechanism. A recent review of the properties of such IF oscillators, particularly at the network level, may be found in Ref. [8]. IF mechanisms are also studied in the context of time-series analysis where they allow reconstruction of attractors from threshold crossing times [10,11]. In more detail we consider an externally forced (nonautonomous) IF oscillator evolving according to the equations

$$\frac{dU}{dt}=f(U,t), \quad f(U,t)=-\frac{U}{\tau}+A(t) \tag{1}$$

subject to reset:

$$U_-(T^n)\equiv\lim_{\delta\to 0}U(T^n-\delta)=1, \quad U_+(T^n)\equiv\lim_{\delta\to 0}U(T^n+\delta)=0. \tag{2}$$

The input function $A(t)$ will be taken to be periodic in time such that $A(t)=A(t+1)$. The firing times are defined as

$$T^n=\inf\{t \mid U(t)\geqslant 1; \quad t\geqslant T^{n-1}\}. \tag{3}$$

An implicit map of the firing times may be obtained by integrating Eqs. (1) between reset and threshold:

$$U_-(T^{n+1})e^{T^{n+1}/\tau}=U_+(T^n)e^{T^n/\tau}+\int_{T^n}^{T^{n+1}}e^{s/\tau}A(s)ds. \tag{4}$$

Introducing the function

$$G(t)=\int_{-\infty}^{0}e^{s/\tau}A(t+s)ds=\frac{e^{-1/\tau}}{(1-e^{-1/\tau})}\int_0^1 e^{s/\tau}A(t+s)ds, \tag{5}$$

so that $G(t)=G(t+1)$, and defining $F(t)=e^{t/\tau}[G(t)-1]$, a map of the firing times can be obtained from Eq. (4) as

$$F(T^{n+1})=F(T^n)+e^{T^n/\tau}. \tag{6}$$

For a constant external input $A(t)=I_0$ and $I_0\tau>1$ the map of the corresponding interspike interval (ISI) $\Delta^n=T^{n+1}-T^n$ has a fixed point with $\lim_{n\to\infty}\Delta^n=\tau\ln[I_0\tau/(I_0\tau-1)]$. For simplicity we consider IF oscillators to have at least a constant input $I_0$, so that in the absence of any other external forcing their behavior will be oscillatory. The case of nonoscillatory behavior may be handled in exactly the same fashion as long as the external forcing is sufficient to produce repetitive output firing patterns. In effect we exclude the study of oscillator death. Our approach is consistent with recent work on the periodically driven FitzHugh-Nagumo neuron model, where Arnold tongues are shown to change continuously when the model switches from excitable to oscillatory behavior [12]. If $F$ is invertible [$F'(t)\neq 0$ for all $t$] and $F^{-1}$ is defined on the range of $F(t)+e^{t/\tau}$, then we have an explicit map of the form

$$T^{n+1}=\Psi(T^n), \quad \Psi(t)=F^{-1}[F(t)+e^{t/\tau}]. \tag{7}$$

If $F$ is not invertible then the mapping $T^n\mapsto T^{n+1}$ is defined according to Eq. (3). This highlights the fact that, in general, the map of firing times is only implicitly available. From Eq. (5) it is easy to establish that $\tau G'(t)+G(t)=\tau A(t)$, so that the condition $F'(t)=e^{t/\tau}[A(t)-\tau^{-1}]\neq 0$ can be guaranteed if $A(t)\neq\tau^{-1}$. Whenever this is the case and $F^{-1}$ is defined on the range of $F(t)+e^{t/\tau}$, one may establish that $F(\Psi(t)+1)=e^{1/\tau}F(\Psi(t))=F(\Psi(t+1))$, and hence that $\Psi(t+1)=\Psi(t)+1$. Indeed, Eq. (7) may now be viewed as the iteration of a circle mapping. Introducing the function $g(t)=\Psi(t)-k$ such that $0\leqslant g(0)<1$ leads to the mapping $T^{n+1}=g(T^n)+k$ with $g(t+1)=g(t)+1$. Introducing

$$\underline{\rho}(t)=\liminf_{n\to\infty}\frac{g^n(t)}{n}, \quad \overline{\rho}(t)=\limsup_{n\to\infty}\frac{g^n(t)}{n} \tag{8}$$

allows the definition of the rotation interval of $g$ as $L(g)=[\rho_-,\rho_+]$, where

$$\rho_-=\inf_{t\in\mathbb{R}}\underline{\rho}(t), \quad \rho_+=\sup_{t\in\mathbb{R}}\overline{\rho}(t). \tag{9}$$

When the rotation interval reduces to a single point, denoted by $\rho$ (so that $\rho_-=\rho_+$), then $\rho$ is called the rotation number of $g$ and the lim sup and lim inf in Eq. (8) can be replaced by a simple limit. The choice of $k$ ensures that $0\leqslant\rho<1$, so that $\rho$ measures an average phase rotation per iteration. If $\rho$ exists and is rational, then there is an initial $T^0$ such that the

sequence $\{T^n \bmod 1\}$ approaches a periodic sequence asymptotically for large enough $n$, i.e., mode locking occurs. However, if $\rho$ is irrational then every solution is ergodic and the sequence $\{T^n \bmod 1\}$ is dense in the interval $[0,1)$ [assuming that $\Psi(t)$ is continuous]. When a nontrivial rotation interval exists, a positive value for the topological entropy is implied. For a detailed account of the possible routes to chaos (or more precisely positive topological entropy) in circle maps, see Ref. [5]. If the explicit map of firing times defined by Eq. (7) is to describe an invertible circle map, we must also have that $\Psi'(t) \neq 0$. Since $\Psi'(t) = A(t) e^{t/\tau}/F'(\Psi)$ this is the case whenever $A(t) \neq 0$. If $A(t)$ is such that $A(t) > \tau^{-1}$ for all $t$, then both $A(t) \neq \tau^{-1}$ and $A(t) \neq 0$ are true simultaneously, and the firing map dynamics can always be reduced to an invertible map of the circle. Chaotic dynamics is not possible in this situation.

### Mode locking

One would expect the IF oscillator to fire one or more spikes at times which are integer multiples of the driving period. This pattern of activity may be considered as a bursting state with interburst intervals mainly influenced by the driving period and intraburst intervals dependent upon system parameter values. With this in mind it is natural to seek mode-locked solutions of the form

$$T^n = \left[\frac{n}{p}\right]\Delta - \phi_{n(p)}\Delta, \quad n(p) = n \bmod p, \tag{10}$$

where $[\cdot]$ denotes the integer part, and the $\phi_{n(p)} \in [0,1)$ denote a collection of firing phases. $\Delta$ is assumed to be rationally related to the forcing period (which we have taken as unity). Such an ansatz was previously discussed by Chow [13] within the context of harmonic locking in two pulse-coupled spike response neurons. Here we show how to analyze such solutions systematically. We distinguish three types of solutions: (i) *simple bursting*, (ii) *skipping*, and (iii) a mixed spike train which combines elements of the first two solutions. Simple bursting is described by $\Delta = 1$ and $p > 1$, while skipping is defined by $\Delta = q$ and $p = 1$, for $q \in \mathbb{Z}$. We define the average firing period $\langle \Delta \rangle$ in terms of the ISI's as

$$\langle \Delta \rangle = \lim_{N \to \infty} \frac{1}{N} \sum_{n=1}^{N} \Delta^n. \tag{11}$$

It is easily established that ansatz (10) describes solutions which satisfy $\langle \Delta \rangle = q/p$ and describe $q{:}p$ mode-locked solutions. When $\langle \Delta \rangle$ is independent of initial conditions and both $q{:}p$ and $q'{:}p'$ solutions can be found, then another mode-locked solution is expected (in some intermediate region of parameters) where the entrainment is $q+q'{:}p+p'$ (at least for the case where the firing map is an invertible circle mapping). An example of a $2{:}3$ mode-locked solution is shown in Fig. 1, where the periodic driving signal is sinusoidal.

From Eq. (6) the $p$ firing phases may be determined by the simultaneous solution of the $p$ equations

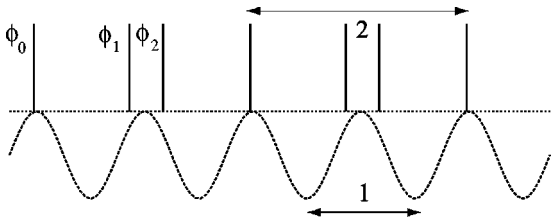


FIG. 1. An example of a $2{:}3$ mode-locked solution that may arise in a sinusoidally forced IF system with $A(t) = 2 + 1.1\sin(2\pi t)$ and $\tau = 1$. Note that the system fires three spikes (with phases $\phi_0, \phi_1$, and $\phi_2$) for every two periods of the driving signal.

$$H_{n(p)}(\Phi,\Delta) \equiv \frac{G(-\phi_{(n+1)(p)}\Delta) - 1}{G(-\phi_{n(p)}\Delta)} - \frac{\exp\frac{\Delta}{\tau}\left(\left[\frac{n}{p}\right] - \phi_{n(p)}\right)}{\exp\frac{\Delta}{\tau}\left(\left[\frac{(n+1)}{p}\right] - \phi_{(n+1)(p)}\right)} = 0 \tag{12}$$

The stability of these solutions may be found by perturbing the firing times such that $T^n \to T^n + \delta^n$ and expanding Eq. (6) to first order in the $\delta^n$'s [assuming $F'(T^n) \neq 0$] around a mode-locked solution. It is convenient to denote a mode-locked solution by the set of phases $\Phi = (\phi_0, \ldots, \phi_{p-1})$ and the period $\Delta$. One may now establish that $\delta^{n+1} = \kappa_{n(p)}(\Phi,\Delta)\,\delta^n$, where

$$\kappa_{n(p)}(\Phi,\Delta) = \exp\left\{-\frac{\Delta}{\tau}\left(\left[\frac{(n+1)}{p}\right] - \phi_{(n+1)(p)} - \left[\frac{n}{p}\right] + \phi_{n(p)}\right)\right\} \frac{A(-\phi_{n(p)}\Delta)}{A(-\phi_{(n+1)(p)}\Delta) - \tau^{-1}}. \tag{13}$$

In particular, a numerical continuation of $q{:}p$ mode-locked solutions is possible from the state with a constant drive where $A(t) = I_0$. In this case the phases are given by $\phi_{n(p)} = 1 - n(p)/p$, and the decay parameter $\tau$ satisfies $I_0\tau = [1 - \exp(-q/(p\tau))]^{-1}$. The persistence of a mode-locked state with $p$ phases and period $\Delta$ depends upon the behavior of the map

$$\delta^{n+1} = \left(\prod_{m=0}^{p-1} \kappa_m(\Phi,\Delta)\right)\delta^{n+1-p}. \tag{14}$$

This has solutions of the form $\delta^n = e^{n\nu/p}$ for $\nu \in \mathbb{C}$. Hence the stability of a mode-locked state is guaranteed for $\mathrm{Re}(\nu(\Phi,\Delta)) < 0$, where

$$\mathrm{Re}(\nu(\Phi,\Delta)) = \ln|\kappa(\Phi,\Delta)| \tag{15}$$

and

$$\kappa(\Phi,\Delta)=\prod_{m=0}^{p-1}\kappa_m(\Phi,\Delta)$$

$$=e^{-\Delta/\tau}\prod_{m=0}^{p-1}\left[\frac{A(-\phi_{m(p)}\Delta)}{A(-\phi_{(m+1)(p)}\Delta)-\tau^{-1}}\right]. \quad (16)$$

If $\kappa(\Phi,\Delta)<0$, then $\omega\equiv \mathrm{Im}(\nu)=\pi$. The borders of the regions where such mode-locked solutions become unstable are defined by the conditions $\mathrm{Re}(\nu(\Phi,\Delta))=0$, where the set of phases $\Phi$ is obtained from the solution of Eqs. (12). Typically, for noninvertible circle maps, the borders of such regions (Arnold tongues) split into two branches in parameter space. Consequently Arnold tongues can cross, leading to a situation in which two or more different periodic orbits associated with different rotation numbers are found at the same parameter values (multistability). The complete Arnold tongue structure is often complex, with borders defined by tangent and period doubling bifurcations. Moreover, beyond the accumulation points of the period doubling sequences there is chaos (in the sense of a positive Liapunov exponent). The systems studied in this paper typically occupy regions of parameter space where the firing times are either described by an invertible circle map or a map of the real line that does not allow a period doubling cascade. In either case chaotic motion is nongeneric and the dynamics is either periodic or quasiperiodic. A study of chaotic motion in IF systems is presented elsewhere [7].

For a classification of the behavior of spike trains, an explicit knowledge of the dynamics is desirable, which suggests working with the original dynamics (1) and (2) that underlies the map of firing times generated by Eq. (3). However, the analysis of IF dynamics is far from trivial owing to the presence of harsh nonlinearities at reset. Recently, techniques originally developed for the study of impact oscillators have been used in the construction of the Liapunov exponent for IF systems, so that the robustness of spike trains may be examined [7]. The Liapunov exponent for the discontinuous dynamical system defined by Eqs. (1) and (2) is derived in Appendix A as

$$\lambda=-\frac{1}{\tau}+\lim_{k\to\infty}\frac{1}{(T^k-T^0)}\sum_{j=1}^{k}\ln\left|\frac{f(0,T^j)}{f(1,T^j)}\right|. \quad (17)$$

There are two contributions to $\lambda$; one from the smooth flow between successive firings, and the other from the discontinuous nature of the resetting mechanism. Hence spike trains may be termed periodic, aperiodic, or chaotic if $\lambda<0$, $\lambda=0$ or if $\lambda>0$ respectively.

## III. MODE-LOCKING IN A PERIODICALLY FORCED IF OSCILLATOR

Return maps constructed from the data generated by a periodically stimulated squid giant axon show that mode-locked dynamics is governed by a one-dimensional deterministic description [14]. Since the IF oscillator is a (possibly quite severe) one-dimensional reduction of the physiologically realistic Hodgkin-Huxley neuron model, it may provide a framework for organizing the behavior seen in real experiments. Indeed, this philosophy has recently been adopted in an analysis of the periodically stimulated FitzHugh-Nagumo neuron model, where the dynamics was described in terms of a one-dimensional map that approximates the Poincaré map of the forced system. The benefit of working with the IF oscillator from the outset is that, as we have just shown, precise statements about the dynamics and Arnold tongue structure can be made without recourse to approximations. Of course, as in many studies of neural systems, one makes a trade-off between biological realism and mathematical tractability. Sinusoidal forcing of IF oscillators was previously analyzed in Ref. [15], although by not using an ansatz for the firing times such as given by Eq. (10) the authors were not able to explore the possibility of constructing Arnold tongues. As well as extending the work on sinusoidally forced IF systems, we also consider the case of periodic pulsatile stimulation that gives rise to post-synaptic potentials with a finite rise and fall times. In both cases borders of the Arnold tongue defined by tangent bifurcations $[\kappa(\Phi,\Delta)=1]$ can occur in the regime where the map of firing times is described by an invertible circle map. In practice the solutions for constant forcing (where the dynamics reduces to that of an invertible circle map) are numerically continued into other regimes of parameter space (where connected solutions can be shown to exist using the implicit function theorem) including the region where the map of firing times is not a circle map.

### A. Sinusoidal forcing

Consider a periodic forcing with $A(t)=I_0+\epsilon\sin 2\pi t$. In this case,

$$G(t)=I_0\tau-\frac{\epsilon\tau}{\sqrt{1+4\pi^2\tau^2}}\sin(\theta-2\pi t), \quad \tan\theta=2\pi\tau. \quad (18)$$

For example, in the case of 1:1 frequency locking the stability of solutions is determined from Eq. (13) by $|\kappa|<1$, with

$$\kappa=e^{-1/\tau}\left[1+\frac{\tau^{-1}}{I_0-\tau^{-1}-\epsilon\sin(2\pi\phi)}\right], \quad (19)$$

where $\phi$ is the solution of $G(-\phi)=(1-e^{-1/\tau})^{-1}$. A necessary condition for defining an explicit firing map of the form of Eq. (7) is that $I_0+\epsilon\sin 2\pi t\neq\tau^{-1}$ for all $t$. This is guaranteed for the choice $I_0-|\epsilon|>\tau^{-1}$. In this case the measure of the parameter set for mode locking goes to zero as $\tau\to\infty$. When $I_0-|\epsilon|<\tau^{-1}$ it is known that mode locking can occur almost everywhere, i.e., for parameter values on the complement of a set of measure zero [15]. These points are illustrated in Fig. 2 where we show the bifurcation sequence of the ISI as a function of $\tau$ for fixed $I_0$ and $\epsilon$. In the regime of noncircle map dynamics (the left hand region of the bifurcation diagram) the IF Liapunov exponent is seen to be always negative, indicating a periodic behavior for the sequence of ISIs or equivalently the existence of mode-locked solutions. After crossing into the region where the map of firing times is a circle map, the Liapunov exponent is either zero (indicating a quasiperiodic behavior) or negative, as expected. To illustrate a possible bifurcation sequence consider the right

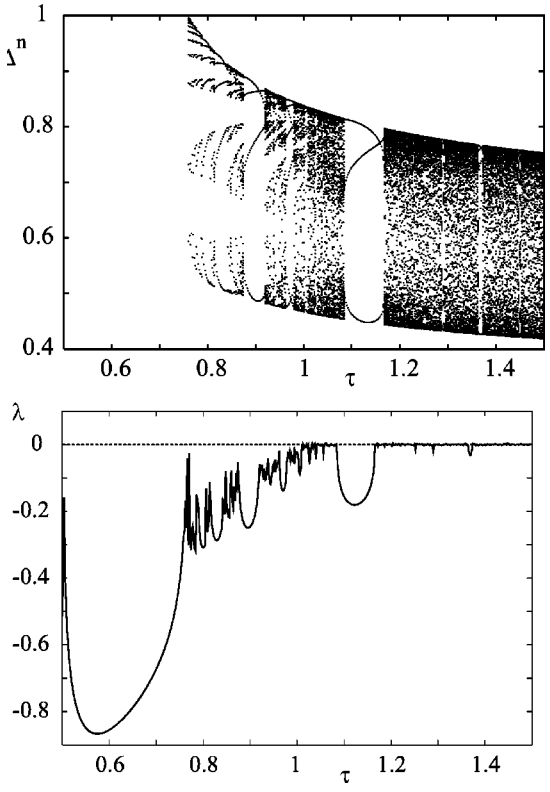


FIG. 2. Top: Bifurcation diagram for the interspike interval $\Delta^n = T^{n+1} - T^n$ as a function of the decay time $\tau$. Bottom: The Liapunov exponent $\lambda$ shows that orbits are either periodic ($\lambda < 0$) or quasiperiodic ($\lambda = 0$). Parameters are $I_0 = 2$ and $\epsilon = 1$. From $\tau = 0.5$ till the first bifurcation point, the system is 1:1 frequency locked with the external signal. Note the transition at $\tau = 1$ ($I_0 - \epsilon = \tau^{-1}$) from a locked regime to one in which a mixture of quasiperiodic and mode-locked behavior may occur. In this regime the measure of the parameter set for mode locking goes to zero as $\tau \to \infty$.

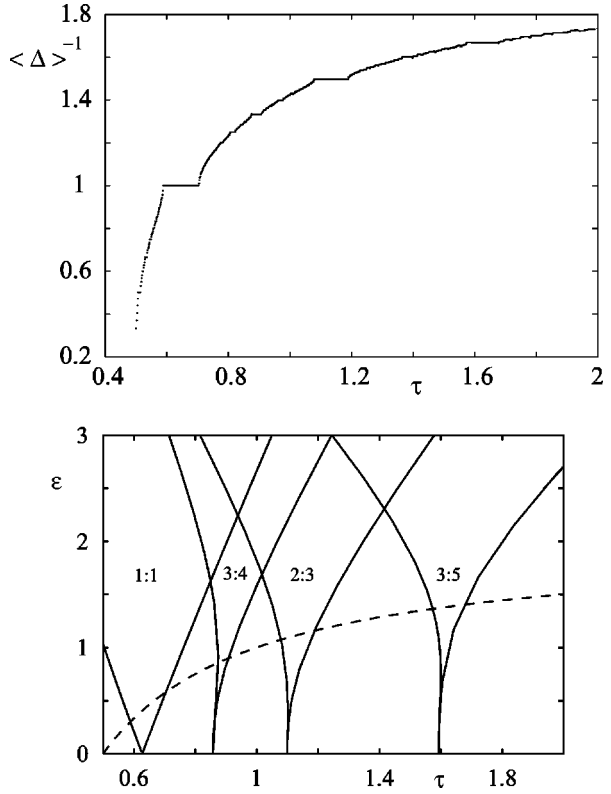


FIG. 3. Top: Plot of the average firing frequency, by directly integrating the IF equations of motion, as a function of the decay parameter $\tau$ for $\epsilon = I_0 - \tau^{-1}$ with $I_0 = 2$ (i.e. along the border between circle map and noncircle map dynamics for the firing times.) Note that the dominant mode solutions are 1:1, 3:4, 2:3, and 3:5 (with increasing $\tau$). In the bottom figure we show the Arnold tongue structure for these dominant modes, predicted from our theoretical analysis. Below the dashed line $\epsilon = I_0 - \tau^{-1}$ a well defined rotation number for the circle map of firing times exists, and the tongues do not overlap.

hand border of stability for the 1:1 mode-locked state shown in the bottom part of Fig. 3 for $\tau \sim 0.65$. As $\epsilon$ increases, a stable-unstable pair of 1:1 mode-locked solutions is created in a tangent bifurcation. At this point the map of firing times is described by an invertible circle map and a well defined rotation number (for the circle map) exists. In the region that is not mode locked (outside the tongue) ergodic dynamics is also possible, since the circle map is invertible. With increasing $\epsilon$ the firing map no longer reduces to dynamics on a circle, although mode-locked solutions continue to exist. Hence the natural quantity to associate with a mode-locked state is the average firing frequency $\langle \Delta \rangle^{-1}$, since rotation numbers can only be defined for restricted regions of parameter space. We plot $\langle \Delta \rangle^{-1}$ as a function of $\tau$ with $\epsilon = I_0 - \tau^{-1}$ (i.e., along the border separating the firing dynamics into a map of the real line and a lift of a map of the circle) in Fig. 3. The resulting devil's staircase structure shows that the preferred mode-locked solutions are those with low ratios of $q$ to $p$. For large $\epsilon$ it is possible for the tongues to overlap (see the bottom part of Fig. 3). In this case mode-locked solutions with different average firing frequencies coexist at a point in parameter space leading to multistability. In numerical simulations the mode-locked solution that is reached will depend upon the basin structure for the coexisting attractors and the choice of initial conditions.

### B. Periodic synaptic input

In neural systems a more realistic input takes the form of a stream of pulses, each of which is convolved with some kernel describing the effects of synaptic and dendritic processing as well as axonal delays [16–18]. For a kernel function $\alpha(t)$ an input stream with period 1 may be written $A(t) = I_0 + \epsilon E(t)$, with $E(t) = \Sigma_{k \in \mathbb{Z}} \alpha(t-k)$, and $E(t)$ is periodic such that $E(t) = E(t+1)$. For synaptic processing the kernel $\alpha(t)$ is often taken to be a difference of two exponentials or more simply a so-called $\alpha$ function with $\alpha(t) = \alpha^2 t \exp(-\alpha t)\Theta(t)$. $\Theta(t)$ is a step function such that $\Theta(t) = 1$ if $t > 0$ and is zero otherwise. Focusing on this typical synaptic kernel we have

$$E(t) = \frac{\alpha^2 e^{-\alpha t}}{(1-e^{-\alpha})}\left[ t + \frac{e^{-\alpha}}{(1-e^{-\alpha})} \right], \quad t \in [0,1). \tag{20}$$

The function $G(t)$ is readily calculated for $t \in [0,1)$ as

$$G(t)=I_0\tau+\frac{\epsilon e^{-1/\tau}}{(1-e^{-1/\tau})}[R(0,1-t,t)+R(1-t,1,t-1)], \tag{21}$$

where

$$R(a,b,t)=\frac{\gamma\alpha^2 e^{-\alpha t}}{(1-e^{-\alpha})}\left\{\left[t+\frac{e^{-\alpha}}{1-e^{-\alpha}}-\gamma\right]\times(e^{b/\gamma}-e^{a/\gamma})+be^{b/\gamma}-ae^{a/\gamma}\right\}, \tag{22}$$

and $\gamma^{-1}=\tau^{-1}-\alpha$. Denoting the maximum value of $E(t)$ as $E^*$, the border between circle map dynamics and noncircle map dynamics is defined by $I_0+\epsilon E^*=\tau^{-1}$ for $\epsilon<0$. In Fig. 4 we plot the average firing frequency of the driven IF oscillator for the case of inhibitory coupling ($\epsilon<0$). This nicely illustrates the possibility of skipping solutions in which the dominant solutions (in the sense of occupying relatively large regions of parameter space) are those which are $q$:1 mode locked. The overlap for the tongues in parameter space where $\epsilon$ is negative and $\alpha$ is large can be considerable (see the bottom of Fig. 4). We have not probed this multistable structure in detail except to note that for random initial data one typically sees a devil's staircase structure for the average firing frequency as a function of $\epsilon$ rather than just the plateaus defined by the overlapping $q$:1 solutions. Once again for the reasons discussed in Sec. II the dynamics is expected to be either periodic or quasiperiodic. This was confirmed numerically by evaluation of the IF Liapunov exponent (not shown).

In both the examples presented here the dynamics may be regarded as belonging to motion on an invariant circle or attractor in the phase space of ISIs. For example, 1:1 mode locking would correspond to a fixed point of the map of ISIs which would manifest itself as a point in a plot of the delay embedding $(\Delta^{n-1},\Delta^n)$. Mode-locked solutions correspond to periodic orbits, as illustrated in the top part of Fig. 5, while very high order or possibly aperiodic ones take the form shown in the bottom part of Fig. 5, which also illustrates the possibility of ergodic behavior on the attractor of the firing map.

## IV. MODE-LOCKING IN A PAIR OF PULSE-COUPLED IF OSCILLATORS

Much is known about the types of phase-locked solutions that can arise in 1:1 frequency locking of two synaptically coupled IF oscillators [16,19]. However, much less is known about the existence and stability of more general $q$:$p$ mode-locked solutions. To date it seems that only a comprehensive study of two linearly weakly coupled integrate-and-fire oscillators has been performed [20]. Here we pursue the more general case of synaptic coupling.

Consider two nonidentical integrate-and-fire oscillators labeled by $i=1,2$, such that neuron 1 couples to neuron 2, and vice versa. We specify these interactions with the aid of a coupling matrix with components $W_{ij}$. In general the equations of motion may be written

$$\frac{dU_i}{dt}=f_i(U_i,t), \quad t\in(T_i^n,T_i^{n+1}), \quad i\neq j, \tag{23}$$

where $f_i(U_i,t)=-U_i+I_i+\epsilon\Sigma_j W_{ij}E_j(t)$. For simplicity we have chosen units of time such that $\tau=1$. As in Sec. III B we consider a synaptic kernel given by an $\alpha$ function so that $E_j(t)=\Sigma_{k\in\mathbb{Z}}\alpha(t-T_j^k)$. Integrating the equations of motion over the interval $(T_i^n,T_i^{n+1})$, subject to reset, yields

$$1=(1-e^{-(T_i^{n+1}-T_i^n)})I_i+\epsilon e^{-(T_i^{n+1}-T_i^n)}\int_0^{T_i^{n+1}-T_i^n}e^t\sum_j W_{ij}E_j(t+T_i^n)dt. \tag{24}$$

In a similar fashion to the analysis of Sec. II, we introduce the following ansatz for the firing times:

$$T_i^n=\left[\frac{n}{p_i}\right]\Delta-\phi_{n(i)}^i\Delta, \quad n(i)=n \mod p_i. \tag{25}$$

These may be regarded as *bursting* patterns where oscillator $i$ fires $p_i$ times in a time $\Delta$ before repeating. For example, one may imagine neuron 1 firing a doublet of spikes in a time-window $\Delta$, whereas neuron 2 might fire a triplet. Note that (by definition) $E_j(t)$ is periodic in $\Delta$. Moreover, it may be written in the form

$$E_j(t)=\sum_{k=0}^{p_j-1}E(t+\phi_{k(j)}^j\Delta), \tag{26}$$

where $E(t)=\Sigma_k\alpha(t-k\Delta)$ and $E(t)=E(t+\Delta)$. Hence, we have $M=p_1+p_2$ equations of the form

$$1=(1-e^{-\Delta_i^n})I_i+\epsilon e^{-\Delta_i^n}\int_0^{\Delta_i^n}e^t\sum_{k=0}^{p_j-1}\sum_j W_{ij}\times E(t+(\phi_{k(j)}^j-\phi_{n(i)}^i)\Delta)dt \tag{27}$$

for $n=0,\ldots,p_i-1$ where $\Delta_i^n=T_i^{n+1}-T_i^n$. By fixing one of the phases we may then solve for the remaining $M-1$ phases and the period $\Delta$. The conditions under which mode-locked or bursting patterns arise in this model for strong coupling are most easily established by considering a reduction to a firing rate or analog model valid in the limit $\alpha\to 0$. Such an approach has previously been used to study the loss of stability of the 1:1 frequency-locked state in networks of two or more IF oscillators [21,22]. In this reduction the average steady state firing rate response of an oscillator is related to the uncoupled ($\epsilon=0$) firing rate function $f(x)^{-1}=\ln[x/(x-1)]\Theta(x-1)$, and the dynamics may be formulated in terms of a set of coupled ordinary differential equations. By choosing $I_i=I-\epsilon f(I)\Sigma_j W_{ij}$ for some $I>1$ it is possible to show that the analog model may undergo a Hopf bifurcation (with increasing $\epsilon$) if the weight matrix $\mathbf{W}$ has a pair of complex eigenvalues. Since periodically time varying firing rates in the analog model correspond to bursting patterns in the IF model, one would therefore expect mode-locked solutions in the full IF model for a mixture of excitatory and inhibitory coupling between oscillators. Indeed, we show a

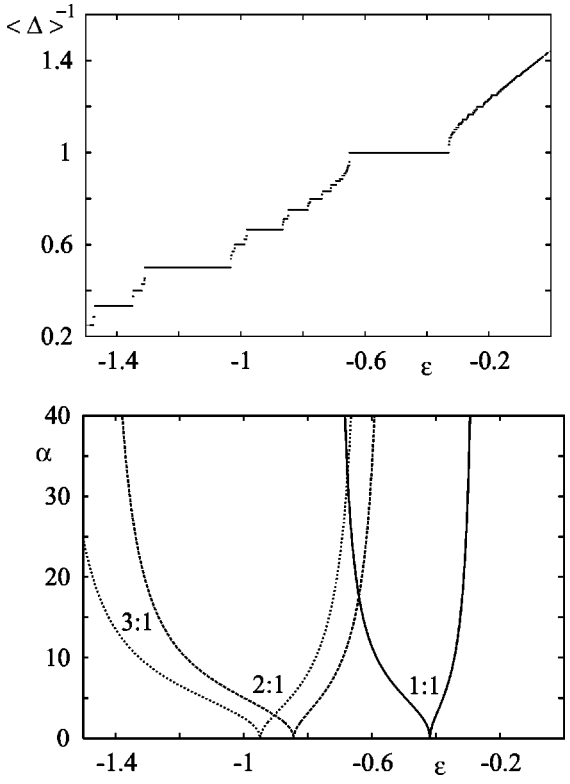


FIG. 4. Numerical experiments show that for $\tau=1$ and $I_0=2$ the synaptically driven IF neuron can easily generate skipping solutions for $\epsilon<0$. The top figure shows the average firing rate in the inhibitory regime for $\alpha=20$, $I_0=2$, and $\tau=1$, illustrating the dominance of the skipping solutions ($q$:1 mode locking). In the bottom figure we plot the theoretically determined borders of stability for such mode-locked solutions in the $(\epsilon,\alpha)$ plane.

numerical example of such behavior in Fig. 6. It is interesting to note that the firing patterns have clearly defined regions of bursting separated by quiescent periods before repeating. This suggests that IF networks support bursting solutions even in the absence of any intrinsic slow calcium like currents often adopted in physiologically realistic neuron models. Other neuronal networks that support bursting in the absence of such currents typically utilize diffusive coupling arising from electrical gap junctions (see Ref. [23] for a discussion).

In order to investigate the linear stability of mode-locked solutions, we consider perturbations $\delta_i^n$ of the firing times. That is, we let $T_i^n \to T_i^n+\delta_i^n$ with $T_i^n$ given by Eq. (25), and integrate Eq. (23) from $T_i^n$ to $T_i^{n+1}$ using the reset condition. This leads to a mapping of the firing times that can be expanded to first order in the perturbations

$$\delta_i^{n+1}-\delta_i^{n+1-p_i} = \epsilon\sum_{m=0}^{p_i-1}\frac{1}{A_i((n-m)(i))}e^{-\Delta_i^{n+m}}\sum_j W_{ij} \times\int_0^{\Delta_i^{n+m}} dt\, e^t\sum_k \alpha'(t-T_j^k+T_i^{n-m})(\delta_j^k-\delta_i^{n-m}), \tag{28}$$

where $A_i(n(i))=I_i-1+\epsilon E_j(-\phi^i_{(n+1)(i)}\Delta)$. Equation (28) has a discrete spectrum that can be found by taking $\delta_j^n=e^{n\lambda/p_j}\delta_j$, $\lambda\in\mathbb{C}$ and $0\leqslant \mathrm{Im}(\lambda)\leqslant 2\pi$. The resulting eigenvalue equation is infinite dimensional, since the dynamics depends upon the whole history of firing times. In the strong coupling regime, it is possible for bifurcations to occur via a Hopf bifurcation in the firing times. This phenomenon has previously been linked to the loss of stability of the 1:1 mode-locked state in networks of two or more IF oscillators [21,22]. Rather than pursue bifurcations in the strong coupling regime, we turn to the limit of weak coupling in which the linear stability analysis becomes considerably more tractable. In this case solutions for $\lambda$ lie in the neighborhood of the real solution $\lambda=0$, or else can be shown to have negative real part [18]. In the limit of zero coupling the firing times occur on a regularly spaced lattice such that $T_i^n=(n-\phi_i)\Delta_i$ where $\Delta_i=\ln[I_i/(I_i-1)]$ and $\phi_i\in[0,1)$ is some arbitrary phase shift. We consider the case in which the periods $\Delta_1$ and $\Delta_2$ are commensurate such that they satisfy $p_1\Delta_1=p_2\Delta_2$. The mode-locking ansatz given by Eq. (25) generates an equivalent set of firing times upon choosing $\phi^i_{n(i)}=1-n(i)/p_i+\phi_i/p_i$ with $\Delta=p_i\Delta_i$. One would expect that for sufficiently weak coupling the firing times will lie close to those generated by the uncoupled system. In fact, averaging theory can be used to predict that this is true for time scales of $O(\epsilon^{-1})$ [18]. For simplicity we restrict attention to the architecture $W_{ij}=1-\delta_{ij}$, since the more general case may be handled in the same fashion as outlined below. By combining the $M$ equations given by Eq. (27), the relative phase $\Phi\equiv\phi_2/p_2-\phi_1/p_1$ can be found from the solution of

$$K(\Phi)\equiv H_1(\Phi)-H_2(-\Phi)=0, \tag{29}$$

where

$$H_i(\Phi)=\sum_{m=0}^{p_i-1}e^{-\Delta/p_i}\int_0^{\Delta/p_i}e^t B_j(t+\Phi\Delta+m\Delta/p_i)dt, \tag{30}$$

$$B_j(t)=\sum_k \alpha(t-k\Delta_j),$$

and $B_j(t)$ is periodic with $B_j(t)=B_j(t+\Delta_j)$. To first order in $\epsilon$ we substitute $\delta_j^n=e^{n\lambda/p_j}\delta_j$ into Eq. (28), and set $\lambda=1$ on the right hand side to obtain

$$\lambda\begin{pmatrix}\delta_1\\ \delta_2\end{pmatrix}=\epsilon\begin{pmatrix}-G_1(\Phi) & G_1(\Phi)\\ G_2(-\Phi) & -G_2(-\Phi)\end{pmatrix}\begin{pmatrix}\delta_1\\ \delta_2\end{pmatrix}, \tag{31}$$

with

$$G_i(\pm\Phi)=\pm\frac{H_i'(\pm\Phi)}{\Delta_i(I_i-1)}. \tag{32}$$

The nonzero eigenvalue is calculated from Eq. (31) as $\lambda=-\epsilon(G_1(\Phi)+G_2(-\Phi))$. The zero eigenvalue merely corresponds to uniform shifts in the phases $\phi_i$ such that the relative phase remains unchanged. Hence in the weak coupling regime the stability for mode-locked solutions with phase $\Phi$ determined from Eq. (29) is determined by

$$\epsilon[H_1'(\Phi)-H_2'(-\Phi)]>0. \tag{33}$$

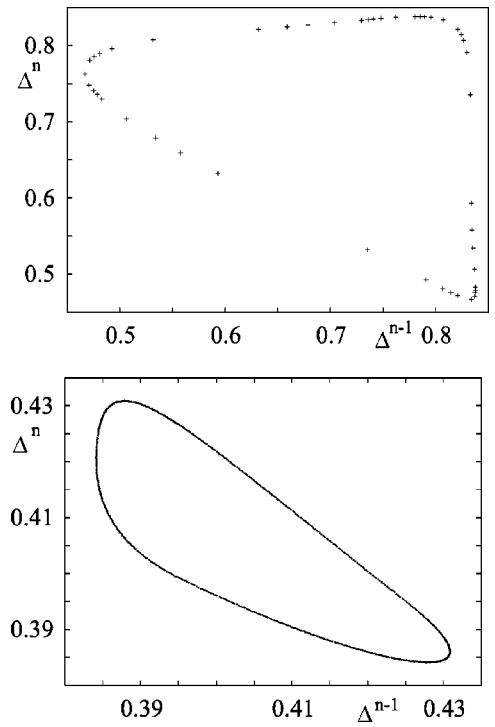


FIG. 5. Top figure: An example of periodic motion on an attracting invariant circle for the ISIs in a sinusoidally forced IF system with $\epsilon=1$, $I_0=2$, and $\tau=1$. Bottom figure: an example of high order periodic motion on an attracting invariant circle for the ISIs in a synaptically forced IF system with $\alpha=2$, $\epsilon=1$, $I_0=2$, and $\tau=1$.

This result is consistent with the one obtained using averaging theory (see Appendix B). Interestingly the expressions we have derived for the existence and stability of mode-locked solutions have the same formal structure as those obtained in studies of weakly coupled limit cycle oscillators where the uncoupled system has a set of hyperbolic stable limit cycles with resonant cycle periods (i.e., they are rationally related to one another). If there are no resonances among the cycle periods, then the system behaves as if it were uncoupled even for nonzero (but small) coupling (see Ref. [24] for a review). For weak coupling only, we have restricted our discussion to the resonant condition $p_1\Delta_1 - p_2\Delta_2=0$, since from the results in Ref. [24] one would not expect mode-locked behavior if this were not the case. In practice a numerical solution for the borders requires an explicit representation for the interaction functions given by Eq. (30). Rather than construct the interaction function $K(\Phi)$ for each $p_1$ and $p_2$ [by explicitly integrating Eq. (30)], it is preferable to work with a closed form expression parametrized by $p_1$ and $p_2$. This is naturally achieved by adopting a Fourier series expansion for $H_i(\Phi)$ (periodic in $1/p_j$), which can be shown to take the form

$$H_i(\Phi)=\frac{(1-e^{-\Delta_i})}{\Delta_j}\sum_{m=0}^{p_i-1}\sum_{n=-\infty}^{\infty}\frac{\tilde{\alpha}(\omega(n,j))}{1+i\omega(n,j)} \times e^{i\omega(n,j)[\Phi\Delta+m\Delta_i]}, \tag{34}$$

where

$$\tilde{\alpha}(w)=\int_{-\infty}^{\infty}e^{-i\omega t}\alpha(t)dt=\frac{\alpha^2}{(\alpha+i\omega)^2}, \quad \omega(n,j)=\frac{2\pi n}{\Delta_j}. \tag{35}$$

An example of the interaction function $K(\Phi)$ is shown in Fig. 7, from which it is also easy to see that the borders of regions in parameter space sustaining mode-locked solutions may be found by solving $\max K(\Phi)=0$ and $\min K(\Phi)=0$. For the 1:1 mode-locked case, $H_1(\Phi)=H_2(\Phi)$, so that, by symmetry, phase-locked solutions with $\Phi=0$ and 1/2 are guaranteed to exist for any values of the system parameters. However, one would expect that when this symmetry condition is violated, as will be the case when $p_1\neq p_2$, then regions in parameter space which support $p_1:p_2$ mode-locked solutions may shrink. This is illustrated in the bottom part of

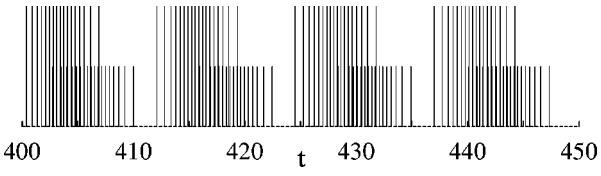


FIG. 6. Example of bursting behavior in a pair of IF oscillators with a mixture of excitatory and inhibitory coupling. $\alpha=0.5$, $I=2$, $W_{11}=W_{22}=0$, and $W_{12}=-W_{21}=1$. Spike trains for the two neurons are distinguished by the height of the spike. Note that both trains may be described by solutions of the form of Eq. (25).

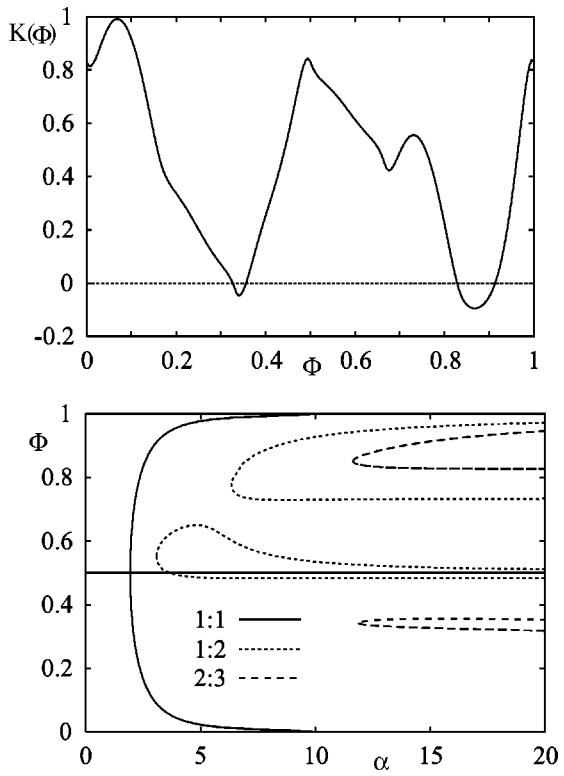


FIG. 7. In the top figure we show a plot of the interaction function $K(\Phi)\equiv H_1(\Phi)-H_2(-\Phi)$ for 2:3 mode locking with $\Delta=2$ and $\alpha=15$. In the bottom figure we show the solutions to $K(\Phi)=0$ for $\Delta=2$ as a function of $\alpha$ for the 1:1, 1:2, and 2:3 mode-locked states. Note that the 1:1 state has solutions for all values of $\alpha$, while all other mode-locked solutions occupy smaller regions of parameter space.

Fig. 7, where it is clearly seen that mode-locked solutions with $p_1 \neq p_2$ satisfying $K(\Phi)=0$ cannot be found for small $\alpha$ (with a fixed $\Delta$).

## V. CONCLUSION

In this paper we constructed Arnold tongues for a periodically forced IF neuron. Our approach was based on a firing map formulation of the dynamics in which the existence and stability of $q:p$ mode-locked solutions for the firing times were derived. In the course of our analysis we highlighted the relationship between mode-locked solutions and bursting states in coupled IF networks, and introduced the notion of a Liapunov exponent that takes into account the presence of discontinuities in the dynamics arising from reset (see also Ref. [7]). There are a number of possible extensions of our work.

(1) In our analysis of a driven IF neuron we restricted ourselves to periodic forcing. An interesting question concerns what happens in response to quasiperiodic or aperiodic signals. A recently highlighted experimental paradigm concerns the measurement of the reliability of spike timing when a neuron is repeatedly stimulated by the same identical time-varying input. It has been demonstrated that spike train reliability is much greater for aperiodic signals than for constant current stimuli [25,26]. Such an effect is found even when variations in the aperiodic signal relative to the dc level are small, as has been demonstrated in experiments on aplysia motorneurons [27]. These experiments have also revealed a resonance effect for neural spike time reliability, in the sense that reliability is enhanced when the spectrum of the input contains a resonant frequency equal to the firing rate of the neuron in response to the dc component. Similar results were obtained for an IF model neuron. One possible measure of spike train reliability (at least for small-amplitude variations in input) is the Liapunov exponent introduced in Appendix A.

(2) When considering aperiodic synaptic inputs, the role of synaptic depression may be important. It has been found that the postsynaptic response of cortical neurons depends on the temporal sequence of action potentials arriving at the presynaptic terminal [28]. This form of short-term synaptic plasticity can lead to an effective reduction in the amplitude of response, and provides a possible mechanism of dynamical gain control [29–31]. The effects of synaptic depression can be incorporated into our analysis of mode-locking in Sec. III B by taking $A(t)=I_0+\epsilon E(t)$ with $E(t)$ defined along the lines of the phenomenological model considered in Refs. [29–31]. This essentially involves the introduction of an amplitude factor $C(T^m)$ that adjusts the magnitude of the response to a spike arriving at time $T^m$ based on previous input history: $E(t)=\Sigma_{m\in\mathbb{Z}} C(T^m)\alpha(t-T^m)$. Following the arrival of a spike at a presynaptic terminal, $C$ is reduced by a multiplicative factor $\gamma<1$ such that $C\to\gamma C$. In between spikes, $C$ is assumed to return to its equilibrium value of one according to the exponential process $\tau_c dC/dt=1-C$ where $\tau_c$ is an appropriately chosen time constant of the order 100 ms. For a given sequence of input firing times $\{T^m, m\in\mathbb{Z}\}$, one finds that $C(T^m)=1+(\gamma-1)\Sigma_{m'<m}\gamma^{m-m'-1}e^{-(T^m-T^{m'})/\tau_c}$. Note that in the special case of periodic synaptic inputs $T^{m+1}=T^m+\Delta$ considered in Sec. III B, the amplitude $C(T^m)$ simply relaxes to its steady-state value $C_\infty=[1-e^{-\Delta/\tau_c}]/[1-\gamma e^{-\Delta/\tau_c}]$, which can be absorbed into the parameter $\epsilon$.

(3) Another important question that we hope to address elsewhere concerns the extent to which the mode-locking behavior exhibited by driven or mutually coupled IF neurons is mirrored by more biophysically detailed models of spiking neurons that also include the effects of noise. For example, it would be interesting to construct ''stochastic'' Arnold tongues for IF neurons along the lines of the recent analysis of the FitzHugh-Nagumo model of a neuron [32].

## ACKNOWLEDGMENTS

The authors would like to thank Bard Ermentrout for making available the software tool XPP, which was used for the numerical continuation of Arnold tongues from the uncoupled state and the construction of mode-locked solutions in the weak coupling regime. This research was supported by Grant No. GR/K86220 from the EPSRC (U.K.).

## APPENDIX A: LIAPUNOV EXPONENT FOR AN IF OSCILLATOR

Introduce a perturbed dynamics $\tilde{U}$ and denote the deviation between perturbed and unperturbed trajectories as $\delta U$. Consider the propagation of an initial perturbation $\delta U(0)$ such that the unperturbed trajectory reaches threshold first. Denoting the time of the $k$th threshold crossing of the unperturbed trajectory as $T^k$, and that of the perturbed trajectory as $T^k+\delta^k$, we have

$$\begin{aligned} 0&=\tilde{U}_-(T^k+\delta^k)-1 \\ &\approx \tilde{U}_-(T^k)+f(\tilde{U}_-(T^k),T^k)\delta^k-1\approx U_-(T^k)+\delta U_-(T^k) \\ &\quad +f(U_-(T^k)+\delta U_-(T^k),T^k)\delta^k-1 \\ &\approx \delta U_-(T^k)+f(U_-(T^k),T^k)\delta^k. \end{aligned} \tag{A1}$$

Hence the perturbation of the firing times is given by

$$\delta^k=-\frac{\delta U_-(T^k)}{f(U_-(T^k),T^k)}. \tag{A2}$$

The difference between the two trajectories just after the perturbed trajectory reaches threshold is

$$\begin{aligned} \delta U_+(T^k+\delta^k)&=0-U_+(T^k+\delta^k) \\ &\approx -f(U_+(T^k),T^k)\delta^k. \end{aligned} \tag{A3}$$

Using Eq. (A2), the perturbations are seen to satisfy

$$\delta U_+(T^k+\delta^k)=\frac{f(0,T^k)}{f(1,T^k)}\delta U_-(T^k). \tag{A4}$$

The same expression is obtained by considering the case when the perturbed trajectory reaches threshold first. In general the Liapunov function for the flow is given by

$$\lambda = \lim_{t\to\infty} \frac{1}{t} \ln \left| \frac{\delta U(t)}{\delta U(0)} \right|, \tag{A5}$$

where the time evolution of $\delta U(t)$ is obtained from a linearizaton of the dynamics. In the IF case with initial condition $\delta U(t_0)$ at time $t_0$ we have, between firing events,

$$\delta U(t) = e^{-t/\tau} \delta U(t_0). \tag{A6}$$

Hence, using Eq. (A4) and (A6), we have that

$$\begin{aligned} \lambda &= \lim_{k\to\infty} \frac{1}{(T^k - T^0)} \ln \left| e^{-(T^k - T^0)/\tau} \prod_{j=1}^{k} \frac{f(0,T^j)}{f(1,T^j)} \right| \\ &= -\frac{1}{\tau} + \lim_{k\to\infty} \frac{1}{(T^k - T^0)} \sum_{j=1}^{k} \ln \left| \frac{f(0,T^j)}{f(1,T^j)} \right|. \end{aligned} \tag{A7}$$

## APPENDIX B: WEAK COUPLING AND AVERAGING

Suppose that in the absence of any coupling, $\epsilon = 0$, each oscillator fires with period $\Delta_i = \Delta/p_i = \ln[I_i/(I_i - 1)]$. Between reset, introduce the nonlinear transform $U_i(t) \to \psi_i(t)$ according to

$$\mod 1 \quad \psi_i(t) + \frac{t}{\Delta_i} = \frac{1}{\Delta_i} \int_0^{U_i(t)} \frac{dU}{(-U_i + I_i)}. \tag{B1}$$

Under such a transformation the dynamics (23) becomes

$$\dot{\psi}_i = \epsilon F_i(\psi_i + p_i t/\Delta) E_j(t), \tag{B2}$$

where

$$F_i(z) = \frac{p_i \exp(\Delta z/p_i)}{I_i \Delta}, \quad F_i(z+j) = F_i(z), \quad j \in \mathbb{Z}. \tag{B3}$$

When $\epsilon = 0$, the phase variables $\psi_i(t) = \psi_i$ are constant in time with periods $\Delta_i$. Hence, there is an attracting 2-torus. The assumption of strong contraction in the neighborhood of the limit cycles enables one to use normal hyperbolicity to predict persistence of a 2-torus which is asymptotically attracting when $\epsilon$ is small. To a first approximation one might suppose that for weak coupling each oscillator fires with a period $\Delta_i$, but that the phase $\psi_i(t)$ drifts slowly according to Eq. (B2). Furthermore, approximating the firing times by $T_j^n = (n - \psi_i(t))\Delta_i$ the right-hand side of Eq. (B2) becomes a $\Delta/p_j$ periodic function of $t$. Since we are concerned with mode-locked solutions which satisfy the resonance condition $p_1\Delta_1 - p_2\Delta_2 = 0$, it is natural to average the right-hand side of Eq. (B2) over $\Delta = p_i\Delta_i$ to obtain a first order normal form for the asymptotic dynamics of equations (B2). Using the periodicity properties of $F_i(z)$, we obtain

$$\begin{aligned} \frac{1}{p_i}\dot{\psi}_i = \frac{\epsilon}{I_i \Delta^2} \sum_{m=0}^{p_i - 1} \int_0^{\Delta/p_i} e^t B_j(t + \Delta(\psi_j/p_j - \psi_i/p_i) \\ + m\Delta/p_i) dt. \end{aligned}$$

Hence, defining $\Psi = \psi_2/p_2 - \psi_1/p_1$, we have

$$\dot{\Psi} = -\epsilon[K_1(\Psi) - K_2(-\Psi)], \tag{B4}$$

where $K_i(\Psi) = e^{\Delta/p_i} H_i(\Psi)/(\Delta^2 I_i)$. Phase-locked solutions satisfy $K_1(\Psi^*) - K_2(-\Psi^*) = 0$. Writing the phase-locked solutions as $\psi_i(t) = \phi_i + p_i \Omega t$ (so that $\Psi^* = \phi_2/p_2 - \phi_1/p_1$), we find that $\Omega$ is an $O(\epsilon)$ contribution to the effective frequency of the oscillators given $\Omega = \epsilon K_1(\Psi^*) = \epsilon K_2(-\Psi^*)$. Linear stability analysis implies that fixed-point solutions are stable if $\epsilon[K_1'(\Psi^*) - K_2'(-\Psi^*)] > 0$.


[1] A. V. Holden, Biol. Cybern. **21**, 1 (1976).
[2] M. R. Guevara, A. Shrier, and L. Glass, Am. J. Physiol. **254**, H1 (1988).
[3] G. A. Petrillo and L. Glass, Am. J. Physiol. **236**, R311 (1984).
[4] R. L. Calabrese and E. de Schutter, Trends Neurosci. **15**, 439 (1992).
[5] R. S. Mackay and C. Tresser, Physica D **19**, 206 (1986).
[6] D. K. Campbell, R. Galeeva, C. Tresser, and D. J. Uherka, Chaos **6**, 121 (1996).
[7] S. Coombes, Phys. Lett. A **255**, 49 (1999).
[8] P. C. Bressloff and S. Coombes, Neural Comput. (to be published).
[9] L. F. Abbott and T. B. Kepler, in *Statistical Mechanics of Neural Networks*, edited by L. Garrido, Lecture Notes in Physics, Vol. 368 (Springer-Verlag, Berlin, 1990), pp. 5–18.
[10] T. Sauer, Phys. Rev. Lett. **72**, 3811 (1994).
[11] D. M. Racicot and A. Longtin, Physica D **104**, 184 (1997).
[12] K. Yoshino, T. Nomura, K. Pakdaman, and S. Sato, Phys. Rev. E **59**, 956 (1999).
[13] C. C. Chow, Physica D **118**, 343 (1998).
[14] D. T. Kaplan, J. R. Clay, T. Manning, L. Glass, M. R. Guevara, and A. Shrier, Phys. Rev. Lett. **76**, 4074 (1996).
[15] J. P. Keener, F. C. Hoppensteadt, and J. Rinzel, SIAM (Soc. Ind. Appl. Math.) J. Appl. Math. **41**, 816 (1981).
[16] S. Coombes and G. J. Lord, Phys. Rev. E **56**, 5809 (1997).
[17] P. C. Bressloff and S. Coombes, Int. J. Mod. Phys. B **11**, 2343 (1997).
[18] P. C. Bressloff and S. Coombes, Physica D **126**, 99 (1999).
[19] C. van Vreeswijk, L. F. Abbott, and G. B. Ermentrout, J. Comput. Neurosci. **1**, 313 (1994).
[20] G. B. Ermentrout, J. Math. Biol. **12**, 327 (1981).
[21] P. C. Bressloff and S. Coombes, Phys. Rev. Lett. **81**, 2384 (1998).
[22] P. C. Bressloff and S. Coombes, Phys. Rev. Lett. **81**, 2168 (1998).
[23] J. Keener and J. Sneyd, *Mathematical Physiology* (Springer, New York, 1998).
[24] F. C. Hoppensteadt and E. M. Izhikevich, *Weakly Connected Neural Networks*, Applied Mathematical Sciences Vol. 126 (Springer-Verlag, Berlin, 1997).
[25] Z. Mainen and T. J. Sejnowski, Science **268**, 1503 (1995).
[26] R. R. D. van Steveninck, G. D. Lewen, S. P. Strong, R.

Koberle, and W. Bialek, Science **275**, 1805 (1997).
[27] J. D. Hunter, J. G. Milton, P. J. Thomas, and J. D. Cowan, J. Neurophysiol. **80**, 1427 (1998).
[28] A. M. Thomson and J. Deuchars, Trends Neurosci. **17**, 119 (1994).
[29] M. V. Tsodyks and H. Markram, Proc. Natl. Acad. Sci. USA **94**, 719 (1997).
[30] L. F. Abbott, J. A. Varela, K. Sen, and S. B. Nelson, Science **275**, 220 (1997).
[31] L. F. Abbott and E. Marder, in *Methods in Neuronal Modelling*, 2nd ed., edited by C. Kock and I. Segev (MIT Press, Cambridge, MA, 1989), pp. 135–169.
[32] A. Longtin and D. R. Chialvo, Phys. Rev. Lett. **81**, 4012 (1998).